A Driving Assistance System with Vision Based Vehicle Detection Techniques

Jyun-Min Dai*, Lu-Ting Wu*, Huei-Yung Lin†, and Wen-Lung Tai‡
*Department of Electrical Engineering
National Chung Cheng University, Chiayi 621, Taiwan
E-mail: g04415052@ccu.edu.tw, b10013108@yuntech.edu.tw
†Department of Electrical Engineering and Advanced Institute of Manufacturing with High-Tech Innovation
National Chung Cheng University, Chiayi 621, Taiwan
E-mail: lin@ee.ccu.edu.tw
‡Create Electronic Optical Co., LTD
Taipei 23557, Taiwan
E-mail: dennydai@create-eop.com.tw

***Abstract*—Lane departure and forward collision detection plays an important role in autonomous driving and commercial driver-assistance systems. This paper presents an integrative approach to vision-based lane departure detection which aims to be as simple as possible to enable the real-time computation while being able to adapt to a variety of highway and urban scenarios on different weather conditions. In this work, we also implement a vision-based forward collision warning system and an overtaking vehicle detection system. The forward collision warning system aims to detect other vehicles driving ahead of the host vehicle so as to avoid the potential traffic accidents. On the other hand, the overtaking vehicle detection system is to detect other vehicles behind or on the side of the host vehicle so as to give an alert to the driver when the vehicle begins overtaking. Experimental results are presented with real scene video sequences. The performance evaluation has demonstrated the effectiveness of the proposed techniques.**

I. Introduction

Nowadays, advanced driving assistance systems (ADAS) have achieved great advances, and several algorithms have been proposed for a better understanding of the environment. They are commonly used to improve the traffic safety and efficiency. Recently, the research on advanced driver assistance systems has gained a great momentum in the vehicle safety issues. Lane departure warning system (LDWS), forward collision warning system (FCWS), and overtaking vehicle detection system (OVDS) are some typical applications of ADAS [1], [2], [3]. LDWS is designed to warn the driver when the vehicle begins to move out of its lane, unless a turn signal is on in the motion direction. FCWS aims to prevent imminent front collision by issuing a warning signal to the driver. The challenges of lane markings and front vehicle detection include the complex road conditions and changing illumination. OVDS is designed to detect the vehicles approaching from the back or either side, and give an alert to the driver. We might not be able to see the cars as quickly as the OVDS on the road or in a parking lot. Meanwhile, robustness and real-time are the key indicators of the system implementation.

Vision-based systems use low-cost cameras as sensing devices. They have attracted considerable attentions in recently years and become very important and practical to the market. This is mainly due to not only its low-cost advantage compared to radar or lidar technologies, but also with the continued advancements and maturity in the image processing techniques. Unlike the radar-based FCWS/OVDS [4], the vision-based systems may further enhance the performance of forward object detection and forward collision warning when combined with object identification and lane detection techniques. When appropriately mounted and calibrated, a vision-based warning system may further be integrated with a lane departure warning system to form a better safety protection to the drivers from both the longitudinal and lateral directions without extra hardware cost.

In recent years, many vision-based system approaches have been proposed [5], [6]. The versatility of vision systems provides rich information like colors, shapes, and depth at low cost without extra power consumption. The previous work on lane detection can be categorized to two different approaches: feature-based and inverse perspective transform-based techniques. The feature-based methods take the road marks [1], [2], [7] or the lane dividing lines [8] as low level features to locate the lane position in the image. The inverse perspective transform-based methods use a linear transformation from the 3D projective space to the 2D projective space [9], [10]. In either case, Hough transform is often used to combine with the road model for lane detection in a short distance range [11]. There also exist other techniques such as using deformable models for lane detection and tracking [12] or using the L-K optical flow method to determine the vehicle's heading angle via the top-view image processing [13]. For the front collision warning, the existing techniques include feature-based [7], stereo-based [14], [15], motion-based [15], [20] and learning-based [16] approaches.

To detect the front vehicle, Lin *et al.* [7] and Chong *et al.* [17] use shadow information underneath a vehicle as a sign pattern for the detection. The shadow detected by grayscale image thresholding [7] or edge gradients [17] are commonly used to locate the front vehicle. Because the area under a

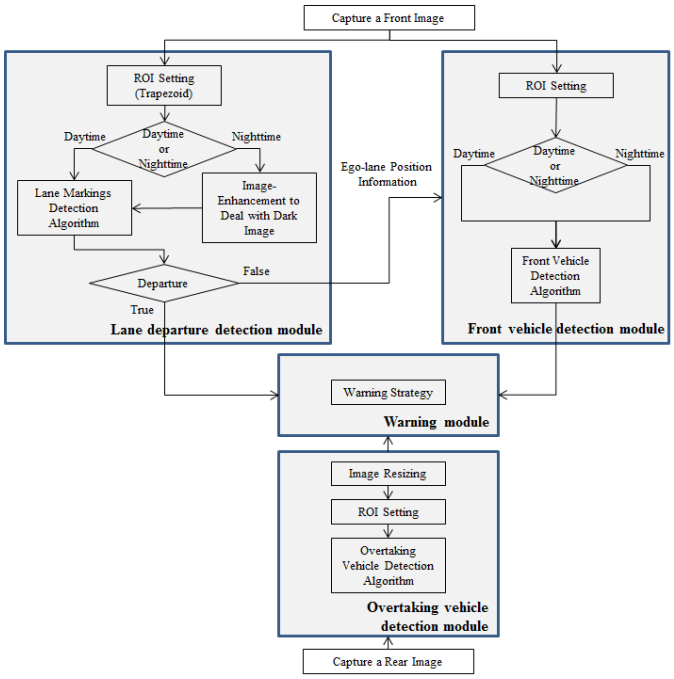

Fig. 1. The flowchart of the entire system.

vehicle is usually distinctly darker than other areas on the road, the vehicle can be located from the position of the cast shadow. However, the intensity of the shadow depends on the illumination of the image, a fixed threshold cannot be used to detect the shadow generally. An adaptive threshold is necessary for a different environment. Furthermore, the shadow features are required to verify whether that is a vehicle or not by training data [18] or symmetry information [19], since the shadow can be easily affected by illumination changes. In [14], the stereo vision system selects reliable features using feature matching and a 3D feature clustering method. It estimates an accurate transform model using a modified RANSAC algorithm for object detection and tracking. Lai *et al.* [15] utilizes the optical flow and regional color feature change to identify the vehicle in the video sequence for their motion-based collision avoidance system. As for the learning-based approaches, Chen *et al.* adopts a multi-layer artificial neural network for robust detection of critical motion from vehicle contextual information [16]. Although the learning-based approach provides better results, it usually has high computational complexity and hardware requirements. Thus, the feature-based approach is adopted in this work.

In the literature of OVDS, Chen *et al.* [21] propose a moving vehicle detection algorithm based on the optical flow estimation of an edge image. The drawback of this method is time-consuming, since it needs to perform the Canny operator on each image frame. Hultqvist *et al.* [22] utilize the 1D optical flow to evaluate along lines parallel to the motion of the overtaking vehicles. The above two methods can easily detect false target because their cameras are mounted on the front of vehicle.

In this study, a vision-based collision warning system that detects the front and overtaking vehicles is proposed. The main objective is to actively warn the driver and provide a real-time notification to avoid possible collisions. We first adopt the method presented by Lin *et al.* [7] to detect the lane departure and front approaching vehicles. Then we propose a new algorithm to improve their drawbacks in complex scenarios. A symmetry analysis technique inspired by [19] is adopted to check whether there is a vehicle in the front. In addition, we develop a motion-based overtaking vehicle detection system using Lucas-Kanade optical flow technique [23]. A road model and an overtaking vehicle model are also established to make system be more robustly.

The techniques presented in this work include a lane departure detection module, a front vehicle detection module, an overtaking vehicle detection module, a warning module to analyze the information from LDWS and FCWS, and two cameras to capture video data from the front view and rear view of the vehicle, respectively. A schematic diagram of the entire system is shown in Fig. 1.

II. Lane Departure Warning System

A. Lane Marking Detection in Daytime

Our lane marking detection algorithm is based on low-level image features. In general, we rarely use the original size of the captured image directly. On the other hand, we usually use only about the half size of the original image after removing the unnecessary regions such as the sky, buildings or traffic signs located in the upper part of the image. Thus, we first define the region of interest (ROI) before performing the lane marking detection algorithm.

Most current methods choose a range above the free space and under the horizon as their ROI for lane marking detection. However, these ROI selections have some disadvantages. For example, it can easily detect the extra information in the both sides of the region, which is generally out of interest especially in the urban areas. To deal with this problem, we pre-set a heuristic trapezoid shaped ROI as shown in Fig. 2. After the ROI selection, Sobel operator is used to calculate the gradient direction of each pixel to restrict the angle. The gradient computation of an image is given by

$$\nabla f = \begin{bmatrix} g_x \\ g_y \end{bmatrix} = \begin{bmatrix} \partial f/\partial x \\ \partial f/\partial y \end{bmatrix}$$

where $\partial f/\partial x$ and $\partial f/\partial y$ are the gradients in the x and y directions, respectively. The gradient direction and magnitude are then calculated by

$$\theta = \tan^{-1}(g_y/g_x) \tag{1}$$

$$G = \sqrt{g_x^2 + g_y^2} \tag{2}$$

where

$$g_x = \begin{bmatrix} -1 & 0 & 1 \\ -2 & 0 & 2 \\ -1 & 0 & 1 \end{bmatrix} \text{ and } g_y = \begin{bmatrix} -1 & -2 & 1 \\ 0 & 0 & 0 \\ 1 & 2 & 1 \end{bmatrix}$$

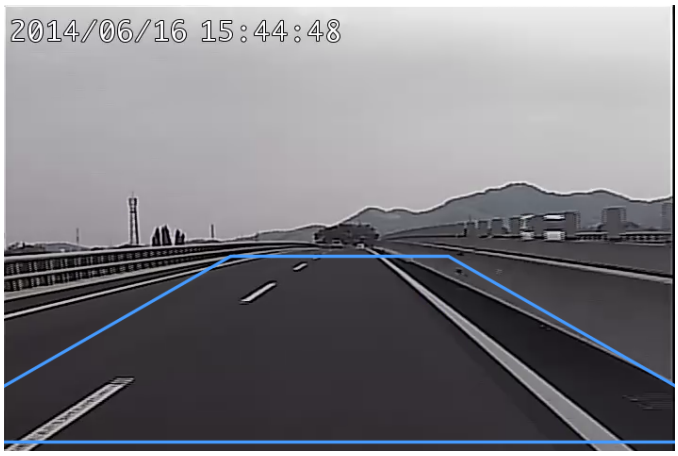

Fig. 2. The proposed heuristic trapezoid shaped ROI.

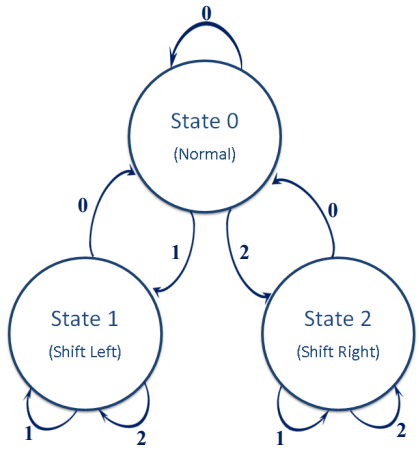

Fig. 4. The state machine for lane departure warning.

In this work, we first restrict the gradient directions from $15°$ to $85°$ and from $95°$ to $165°$ for the left and right lane markings, respectively. This can suppress the horizontal and vertical lines because most of the lane dividing lines in the images are shown in oblique. The gradient magnitudes are used to generate a gradient map. It serves as the input to detect the lane dividing lines. To detect the driving lanes, the gradient image is binarized to an edge image for line detection. In general, the image regions have different characteristics for the scenes associated with different distances. For instance, the intensity variation could be larger for distant scenes. To mitigate this problem, the input image is partitioned into three parts– upper, middle and lower regions, and different thresholds are used to derive the proper edge images. The connected component labeling (CCL) algorithm [24] is then applied to reduce the noise from the oblique line detection after the binary image is generated.

We use Hough transform for line detection with the orientation constraints specified by the vanishing point obtained from the parallel lines in the perspective imaging geometry. In the polar Hough parameter space, we are seeking for the variable r in the equation

$$r = x\cos\theta + y\sin\theta \tag{3}$$

where θ is given by (1). The image pixels on the dividing lanes can then be derived by

$$x = (r - y\sin\theta)/\cos\theta$$

Using the locations of detected lines in the images, the lane departure status includes *left*, *right* and *normal*, as illustrated in Fig. 3. The green line near the bottom of the image shows the wheel location of the vehicle. For the real scene applications, it is unavoidably to have false alarms due to subtle changes in the image or miss detections of the lanes. To increase the accuracy and robustness of our lane departure warning module, a finite state machine as shown in Fig. 4 is implemented. In the proposed system, only the "normal" state can change to "shift right" or "shift left" states, and generate a warning signal. The experimental results demonstrate that this approach can successfully reduce the false alarms due to the lane dividing lines occasionally occluded by other vehicles.

B. Image-enhancement for Low-light Scenarios

We propose a variant of gamma-correction (VGC) function to solve the problems associated with the lack of light sources or dark places. The traditional gamma-correction (TGC) function is a nonlinear operation used to encode and decode luminance or tristimulus values in video or still image systems [25]. It is defined by the power-law expression

$$V_{out} = C \cdot V_{in}^{\gamma} \tag{4}$$

where C is a constant and the input (V_{in}) and output (V_{out}) are non-negative real values.

In the image processing tasks, inputs and outputs are typically in the range of 0 to 255. Thus, we need to generalize the constant C as $C = 255/255^{\gamma}$ where the gamma value γ is less than 1. This process modifies the value of each pixel to make it higher than its original intensity value. The effect of gamma-correction on an image for the gamma value smaller than 1 can make the dark regions brighter. We employ the VGC function, instead of TGC, to calculate the value of each pixel. The equation and rules are defined as follows:

$$V_{out} = \begin{cases} V_{in} \cdot V_{in}^{\gamma}, & \text{if } V_{in} \leq T \\ (\lfloor V_{in} \cdot V_{in}^{\gamma} \rfloor) - 256, & \text{otherwise.} \end{cases} \tag{5}$$

In (5), the constant C is changed to V_{in} since we want to detect the lane markings in dark conditions. The intensity values in the low-light scenarios are usually under about 50, so we set the threshold T as 52. In the experiments, the gamma value is set as $\gamma = 0.4$. Therefore, if V_{in} is greater than the threshold (T), we first round down $V_{in} \cdot V_{in}^{\gamma}$ to the nearest integer value, and then subtract the size of the 8-bits dynamic range of the gray level. Some results are demonstrated in Fig. 5.

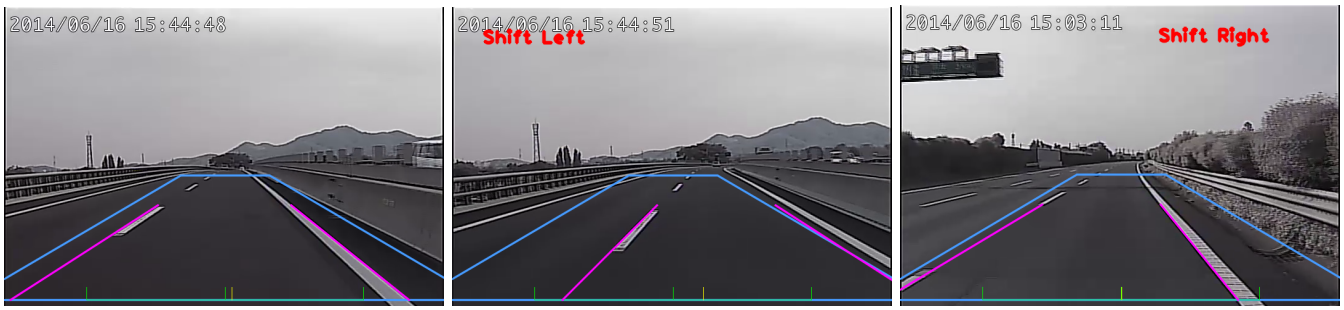

Fig. 3. Lane departure status. Left: normal. Middle: shift left. Right: shift right.

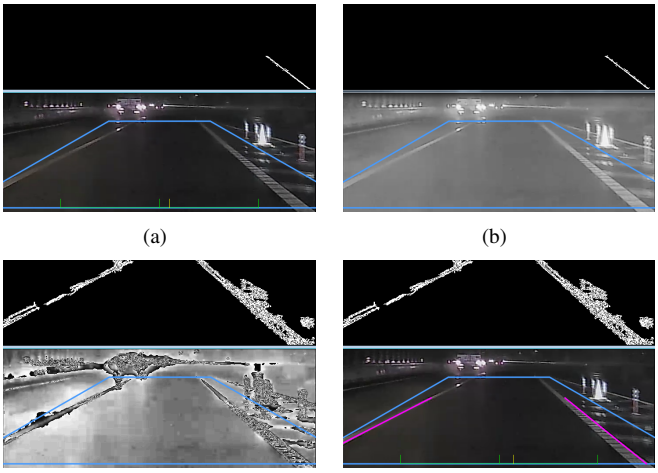

(a) (b) (c) (d)

Fig. 5. Comparison of TGC and VGC results. (a) The result of no use TGC; (b) The result of use TCG; (c) The image of use VGC; (d) The result of use VGC.

III. Forward Collision Warning System

A. Front Vehicle Detection in Daytime

We utilized the shadow underneath vehicle as our feature to help us to detect the front vehicle, because it is the most important feature in the daytime. The front vehicle detection algorithm in the daytime is based on low-level image features. In this paper, we propose the combination of an adaptive ROI and a fixed trapezoid shaped ROI for vehicle detection. The adaptive ROI is located above the fixed trapezoid shaped ROI. We first calculate a 1-D spatial gradient in the y direction and then conduct the image binarization as shown in Fig. 6(a). The adaptive ROI in the figure is related to the width of the vehicle's vertical edge pair.

In the morphological image processing, we define our own 3×3 and 11×11 convolution masks for erosion and dilation, respectively. The convolution masks are shown in Fig. 7. After the erosion and dilation process, we can have the result as demonstrated in Fig. 6(b). The histogram of the vertical projection is then used to detect the vertical edge pair. Before conducting the vertical projection computation, we pre-define several intervals with different width. This is due to not only the vertical edges of the vehicle which can be detected, but also the vertical edges of the scene can be detected easily. The pre-definition different width intervals on the vertical projection map can avoid the influence of noise, and a result is illustrated in Fig. 6(c).

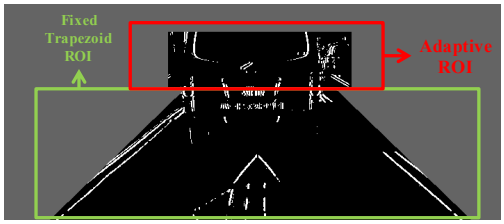

(a) Combination of two different ROIs.

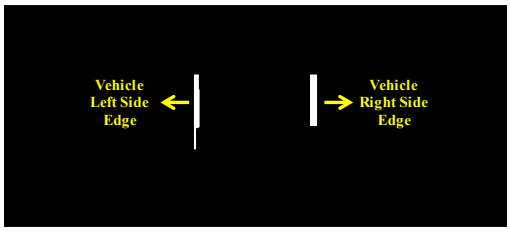

(b) Morphological image processing.

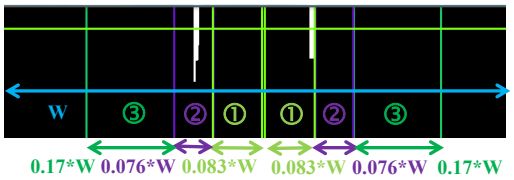

(c) Histogram of vertical projection.

Fig. 6. The detection results of the vertical edge pair.

0	1	0
0	1	0
0	1	0

(a)

0	0	0	1	1	1	0	0	0
0	0	0	1	1	1	0	0	0
0	0	0	1	1	1	0	0	0
0	0	0	1	1	1	0	0	0
0	0	0	1	1	1	0	0	0
0	0	0	1	1	1	0	0	0
0	0	0	1	1	1	0	0	0
0	0	0	1	1	1	0	0	0
0	0	0	1	1	1	0	0	0

(b)

Fig. 7. The mask for the morphological image processing.

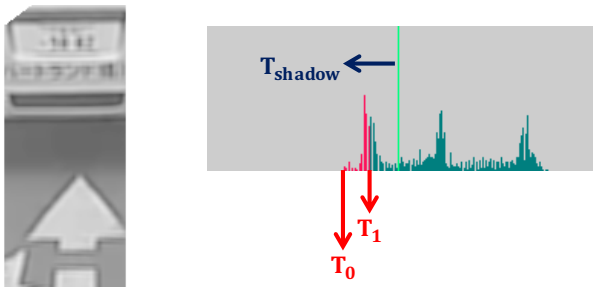

(a) (b)

Fig. 8. The results of the ROI and histogram. (a) The ROI of the CDF calculation; (b) The histogram of the counting numbers of intensity values in each pixel.

To detect the location of the front vehicle, we search the under-vehicle shadow using the cumulative density function (CDF) given by

$$PC_i = No.\ of\ \{p|I(p) = i\}, \quad 0 \leq i \leq 255, \tag{6}$$

$$PA_i = [\Sigma_{j=0}^{i} PC_j]/p_{total} \tag{7}$$

where PC_i is the counting number of intensity values in each pixel within the ROI, p is the pixel within the ROI, $I(p)$ is the intensity values of each pixel, p_{total} is the total number of pixels in the ROI, and PA_i is the percentage of counting numbers of intensity values in each pixel. The ROI of the CDF calculation is demonstrated in Fig. 8(a).

Based on the empirical observation, under-vehicle shadows lie in the range of 0.5% to 15%. Thus, if PA_i exceeds or equals to 0.5% for the first time, we can save T_0 as the location of the intensity value. Similarly, if PA_i exceeds or equals to 15% for the first time, we can save T_1 as the location of the intensity value. Subsequently, a threshold of the under-vehicle shadow (T_{shadow}) as illustrated in Fig. 8(b) is computed by

$$T_{shadow} = T_0 + ((T_1 - T_0) \cdot 3/5) \tag{8}$$

After obtaining the threshold of the shadow, we use it to detect the under-vehicle shadow. The image binarization and morphological image processing are carried out, and connected component labeling is then used to reduce the noise. A result of the image binarization is shown in Fig. 9(a). Then, we calculate the horizontal projection from shadow detection and use it to measure the distance of the front vehicle. Fig. 9(b) shows the derived horizontal projection. The lane width and horizontal projection are updated and checked continuously to see if the shadow in the lane is reasonable or not. It is verified through the following rule:

$$(W_{lane}/3) < L_{hp} < (W_{lane} \cdot 2/3) \tag{9}$$

where W_{lane} is the lane width and W_{hp} is the length of the horizontal projection.

Upon the derivation of the under-vehicle shadow and the width of the vehicle via vertical edge pair detection, the front object location is still unknown. To solve this problem, we propose a solution based on symmetry detection using SURF

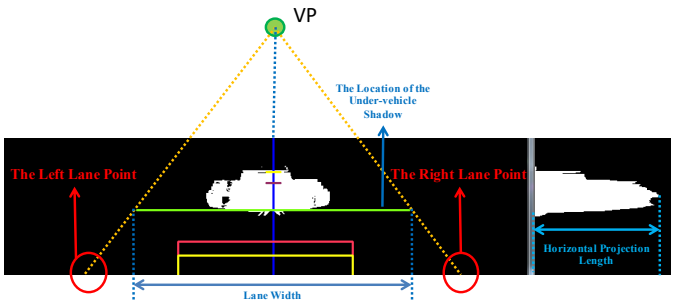

(a) (b)

Fig. 9. The results of the shadow detection. (a) The image binarization of the under-vehicle shadow. (b) The result of the horizontal projection.

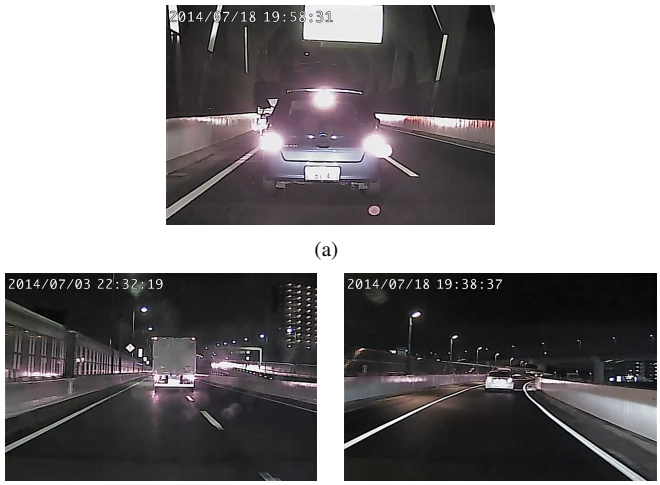

(a)

(b) (c)

Fig. 10. The rear part of the front vehicle affected by lighting affected in nighttime.

feature. First, the width of the vehicle is used to calculate the height of vehicle given by

$$Tp_{vehicle} = Bt_{shadow} + [(R - L) \cdot ratio] \tag{10}$$

where $Tp_{vehicle}$ is the height of the vehicle, R is the location of the vehicle's right side edge, L is the location of the vehicle's left side edge, and the ratio is set as 1.1.

B. Front Vehicle Detection in Nighttime

Our test data was recorded by the LDR vehicle driving recorder. Thus, when the tail lights at night in front of the host vehicle exceeded the range of the photosensitive element that can be stored. It will lead to the tail lights in the image displayed as saturation. Since the driving recorder can not distinguish the difference in the degree of brightness, it causing light rays around the tail lights also displayed as saturation, as illustrated in Fig. 10(a). In addition, the reflected light generated by the headlight irradiating on the rear bumper and the tailgate of the front vehicle. It also cause camera to saturate in places, as shown in Fig. 10(b) and Fig. 10(c).

Fig. 11. Detection of the height of the brightest light area. (a) The inverted V-shaped ROI. (b) The average intensity value of the histogram for each row. (c) The average intensity value of the histogram for each row per 5 frames.

Based on these characteristics, we propose the front vehicle detection algorithm in the nighttime. Firstly, we define the inverted V-shaped ROI in the pre-processing stage, and use the (4) to conduct the decoding gamma for the ROI. Therefore, we set the gamma value as: $\gamma = 2$, as illustrated in Fig. 11(a). Then, we calculate the average of intensity value for each row in ROI as the length of the histogram, as shown in Fig. 11(b). After that, we can find the maximum peaks from a histogram as the position of the brightest area in the ROI. However, in order to suppress the influence which is the road surface reflection in ROI, we take the intensity value for each row to calculate the average over several frames. The suppressing effect is shown in Fig. 11(c).

After we known the height of the brightest area as demonstrated in Fig. 12(a), we can define a new ROI and divide the ROI into four equal portions, as shown in Fig. 12(b). Therefore, we used an adaptive threshold for each ROI is presented in Fig. 12(c). Subsequently, we counted the number of white pixels in each divided regions, and furthermore we kept the divided region of the maximum counting numbers, otherwise removed the remaining regions. The result is illustrated in Fig. 12(d). After getting the result from the Fig. 12(d), we can roughly know the vehicle width. Therefore, we can use the brightest area height and vehicle width informations to define a search area, and the purpose of the search area is in order to detect the lower edge of the rear bumper. The search area is shown in Fig. 13(a).

To detect the location of the front vehicle in nighttime, we detect the lower edge of the rear bumper by using (6) and (7). Based on the empirical observation, when PA_i exceeds or equals to our setting 5%, we let the location of the intensity value i as our threshold value to detect the lower edge of the rear bumper. The histogram of search area is demonstrated in Fig. 13(b). Fig. 13(c) shows the result of the image binarization, then we filter out the noise by morphological processing. Next, we detect the vehicle width is determined by the leftmost and rightmost linked binarization response pixels, and its result is shown in Fig. 13(d). After we obtain the values both of the brightest area height and vehicle width, we can draw the region of the front vehicle such as shown in Fig. 13(e).

IV. Overtaking Vehicle Detection System

The proposed overtaking vehicle detection system from the rear-view consists of four stages: (i) dynamic image acqui-

(a) The height of the brightest area.

(b) The result of the ROI partition.

(c) The result of the image adaptive thresholding.

(d) The results of the maximum counting region.

Fig. 12. Calculation of the roughly vehicle width.

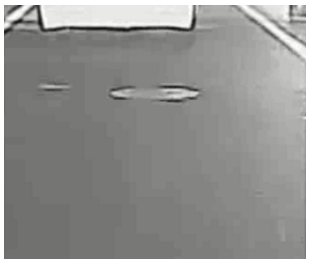

(a) The search area.

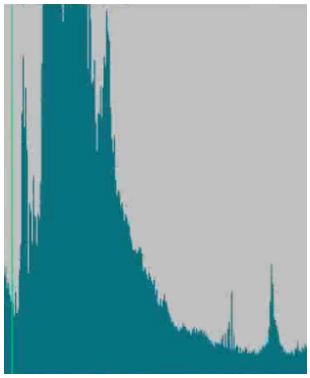

(b) The histogram of search area.

(c) The result of the image binarization.

(d) The result of the image morphological processing.

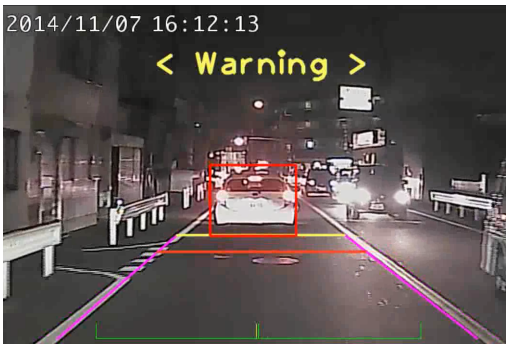

(e) The region of the front vehicle.

Fig. 13. Calculation of the vehicle rear part region from the vehicle aspect ratios.

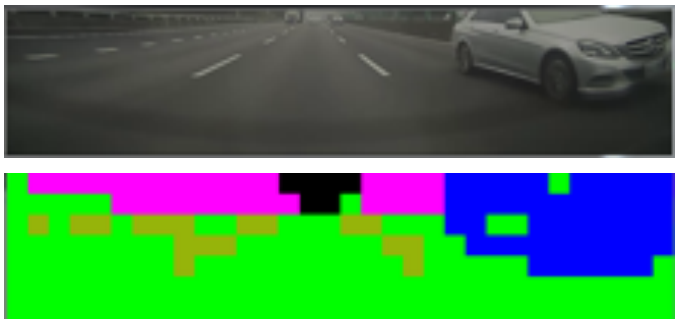

Fig. 14. The pavement, land marking, object approaching from the side and object further away are shown in green, yellow, blue and pink, respectively . The black part represents the uncertain region.

sition and pre-processing, (ii) moving object segmentation, (iii) moving object recognition, (iv) moving object tracking. A single camera is mounted on the rear windshield at 1 meter height. To process the image in real time, a sub-image region of 640×140 pixels is extracted from the original image (with a resolution of 640×400 pixels) for further processing. We first set the feature point selection for a 20×20 image region, and then use the pyramid model of Lucas-Kanade optical flow to calculate the optical flow information of the feature point set. The results are divided into five categories in the motion direction: (i) pavement, (ii) land marking, (iii) overtaking vehicle, (iv) object further away, (v) uncertain region. The results are shown in Fig. 14.

Suppose a vehicle moving forward, a large optical flow will be around the vehicle. On the other hand, the pavement is smooth so the optical flow is small. Therefore, if the optical flow of a feature point is very small, we assign it as the pavement region. If the optical flow in the y direction is very large and moves to the vanishing point, we assign it as the land marking. If the optical flow in the x direction is large and moves far away from the vanishing point, we assign it as the object approaching from the side. Otherwise, we will classify the situation as the object moving further away. In the situation when all the above conditions do not hold, the region is treated as uncertain.

V. Experimental Results

The proposed techniques for LDWS, FCWS and OVDS have been tested on a PC-based platform. Two vehicle driving recorders, CM068A and CB034B, developed by Create Electronic Optical are mounted behind the front windshield and rear windshield, respectively. The video sequences are captured during driving and processed off-line to verify the performance of our techniques. Fig. 15 to Fig. 17 illustrate some results of lane departure and front collision warnings, and overtaking vehicle tracking. It also shows some test video frames used in the performance evaluation, which cover a variety of illumination conditions such as sunny, cloudy or rainy weather, in a tunnel, or during the night time.

Our processing platform is a standard PC with Windows 7 Professional OS, Intel CPU of 3.60 GHz. The computation

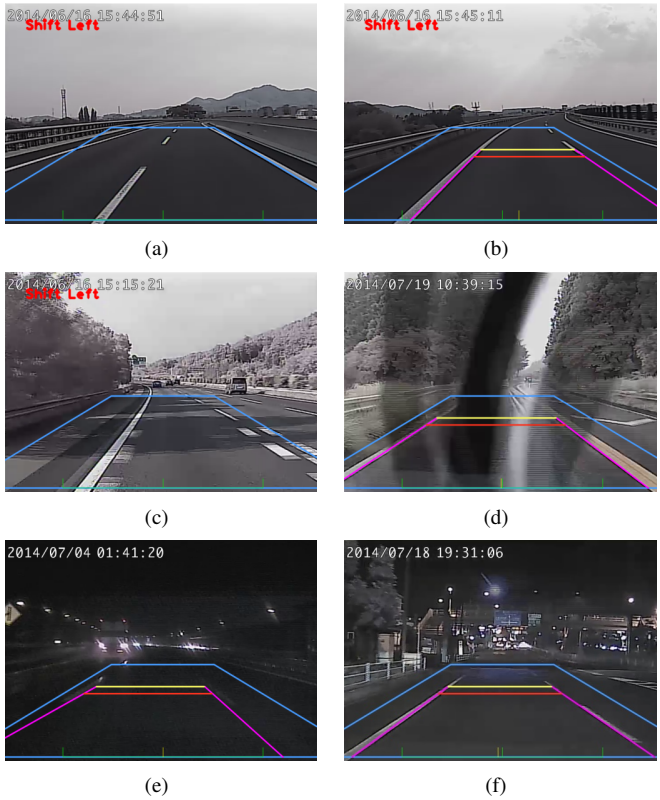

Fig. 15. The results of lane departure warning system.

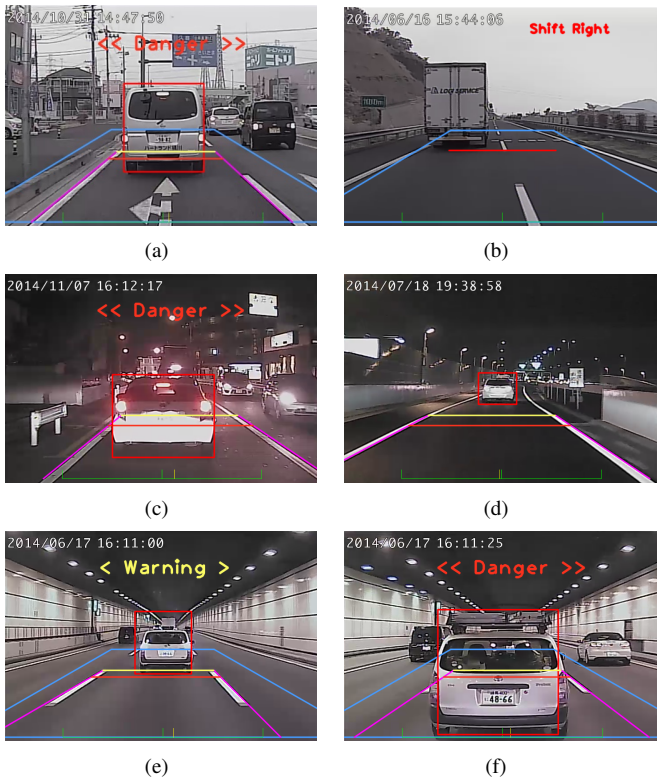

Fig. 16. The results of front collision warning system.

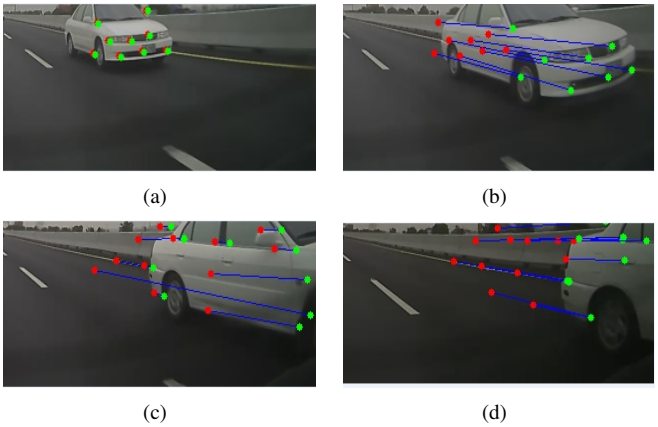

Fig. 17. The tracking results of the overtaking vehicles detection system.

TABLE I
THE PRECISION AND RECALL OF LDWS AND FCWS. T.P.: TRUE POSITIVE, F.P.: FALSE POSITIVE, F.N.: FALSE NEGATIVE.

Test Video	T.P.	F.P.	F.N.	Precision	Recall
LDWS	2423	53	80	97.9%	96.8%
FCWS	1510	0	911	100%	62.4%
OVDS	40	0	2	100%	95.2%

environment is Microsoft Visual Studio 2012 Ultimate, with OpenCV 2.4.9. For the evaluation of lane departure warning system and forward collision warning system, there are totally 2738 and 3464 images respectively. The precision and recall are tabulated in Table I. In the experiments overtaking vehicle detection, we use a driving recorder to capture the dynamic images. There are totally 42 image sequences collected in our database. The success rate of overtaking vehicles detection system with the processing region size of 640×140 is shown in Table I. The execution times per frame for LDWS, FCWS and OVDS are 11.33, 15.46 and 17.38 ms, respectively.

VI. CONCLUSIONS

In this paper, we propose a vision-based driver assistance and warning system for both highway and urban traffic environments. Two single camera driving recorders are used to acquire the traffic scenes for processing. Three subsystems, lane departure warning system (LDWS), front collision warning system (FCWS) and overtaking vehicle detection system (OVDS) are developed. In the performance evaluation on various illumination conditions, our techniques are able to achieve 97.9% of precision on lane departure warnings, and 100% for both the front collision warnings and overtaking vehicle detection.

ACKNOWLEDGMENT

The support of this work in part by Create Electronic Optical Co., LTD, Taiwan, is gratefully acknowledged.

REFERENCES

[1] B.-F. Wu, Y.-H. Chen, C.-C. Kao, Y.-F. Li and C.-J. Chen, "A Vision-Based Collision Warning System by Surrounding Vehicles Detection," *KSII Transactions on Internet and Information Systems,* vol. 6, no. 4, pp. 1203-1222, Apr. 2012.

[2] V. Gaikwad and S. Lokhande, "Lane Departure Identification for Advanced Driver Assistance," *IEEE Transactions on Intelligent Transportation Systems,* vol. 16, no. 2, pp. 910-918, Apr. 2015.

[3] S. Pan and H. Liu, "Detection of Overtaking Vehicles in a Highway," *Proceedings of 2013 Chinese Intelligent Automation Conference,* vol. 256, pp. 163-172, Jun. 2013.

[4] K. Takagi, K. Morikawa, T. Ogawa, M. Saburi, "Road Environment Recognition Using On-vehicle LIDAR," *IEEE Intelligent Vehicles Symposium,* pp. 120-125, Jun. 2006.

[5] S. Sivaraman, "Vehicle detection by independent parts for urban driver assistance," *IEEE Trans. on Intelligent Transportation Systems,* vol. 14, pp. 1597-1608, Dec. 2013.

[6] J.-S. Pan, S. MA, S.-H. Chen and C.-S. Yang, "Vision-based Vehicle Forward Collision Warning System Using Optical Flow Algorithm," *Journal of Information Hiding and Multimedia Signal Processing,* vol. 6, no. 5, pp. 1029-1042, Sep. 2015.

[7] H.-Y. Lin, L.-Q. Chen, Y.-H. Lin and M.-S. Yu, "Lane Departure and Front Collision Warning Using a Single Camera," *IEEE International Symposium on Intelligent Signal Processing and Communication System,* pp. 64-69, Nov. 2012.

[8] J.-W. Hsieh, S.-H. Yu, Y.-S. Chen, and W.-F. Hu, "Automatic traffic surveillance system for vehicle tracking and classification," *IEEE Intelligent Transportation Systems,* vol. 7, no. 2, pp. 175-187, Jun. 2006.

[9] Y. Zhou, R. Xu, X. Hu, and Q. Ye, *A robust lane detection and tracking method based on computer vision,* 2006 IOP Publishing Ltd, Vol. 7, pp. 62-81, Feb. 2006.

[10] J. Huang, H. Liang, Z. Wang, T. Mei, Y. Song, "Robust lane marking detection under different road conditions," *IEEE International Conference on Robotics and Biomimetics (ROBIO),* pp. 1753-1758, Dec. 2013.

[11] A. Suzuki, N. Yasui, N. Nakano and M. Kaneko, "Lane Recognition System for Guiding of Autonomous Vehicle," *Intelligent Vehicles'92 Symposium,* pp. 196-201, Jun. 1992.

[12] Y. Wang, E. K. Teoh, and D. Shen, "Lane detection and tracking using B-Snake," *Image and Vision Computing,* Vol. 22, No. 4, pp. 269-280, Apr. 2004.

[13] G. Taubel and J. S. Yang, "A lane departure warning system based on the integration of the optical flow and hough transform methods," *IEEE International Conference on Control and Automation (ICCA),* pp. 1352-1357, Jun. 2013.

[14] Y.-C. Lim and M. Kang, "Stereo vision-based visual tracking using 3D feature clustering for robust vehicle tracking," *Informatics in Control, Automation and Robotics (ICINCO),* vol. 2, pp. 788-793, Sep. 2014.

[15] Y.-K. Lai, Y.-H. Huang, and C.-M. Hwang, "Front moving object detection for car collision avoidance applications," *IEEE International Conference on Consumer Electronics (ICCE),* pp. 367-368, Jan. 2016.

[16] D.-Y. Chen, J.-J. Wang and C.-H. Chen "Video-based intelligent vehicle contextual information extraction for night conditions," *Machine Learning and Cybernetics (ICMLC),* vol. 4, pp. 1550-1554, Jul. 2011.

[17] Y. Chong, W. Chen, Z. Li, W. H. K. Lam and C. Zheng, "Integrated real-time vision-based preceding vehicle detection in urban roads," *Advanced Theory and Methodology in Intelligent Computing,* vol. 116, pp. 144-149, Sep. 2013.

[18] H. Wang and H. Zhang, "A Hybrid Method of Vehicle Detection based on Computer Vision for Intelligent Transportation System," *International Journal of Multimedia and Ubiquitous Engineering (IJMUE),* vol. 9, no. 6, pp. 105-118, Jun. 2014.

[19] J.-W. Hsieh, L.-C. Chen and D.-Y. Chen, "Symmetrical SURF and its Applications to Vehicle Detection and Vehicle Make and Model Recognition," *IEEE Trans. on Intelligent Transportation System,* vol. 15, no. 1, pp. 6-20, Feb. 2014.

[20] Naito, T. Ito, and Y. Kaneda, "The Obstacle Detection Method using Optical Flow Estimation at the Edge Image," *Intelligent Vehicles Symposium,* pp. 817-822, Jun. 2007.

[21] Y. Chen and Q. Wu, "Moving vehicle detection based on optical flow estimation of edge," *Natural Computation (ICNC),* pp. 754-758, Aug. 2015.

[22] D. Hultqvist, J. Roll, F. Svensson, J. Dahlin, T.B. Schon, "Detecting and positioning overtaking vehicles using 1D optical flow," *IEEE Intelligent Vehicles Symposium Proceedings,* pp. 861-866, Jun. 2014.

[23] J.-Y. Bouguet, "Pyramidal Implementation of the Lucas Kanade Feature Tracker Description of the Algorithm," technical report, Intel Microprocessor Research Labs, 1999.

[24] L. He, Y. Chao and K. Suzuki, "A Run-Based Two-Scan Labeling

Algorithm," *IEEE Transactions on Image Processing,* vol. 17, no. 5, pp. 749-756, May 2008.

[25] C. A. Poynton, *Digital Video and HDTV: Algorithms and Interfaces,* Morgan Kaufmann, pp. 260-630. ISBN 1558607927, 2003.